

# Large Scale Enrichment and Statistical Cyber Characterization of Network Traffic

Ivan Kawaminami<sup>1</sup>, Arminda Estrada<sup>1</sup>, Youssef Elsakkary<sup>1</sup>, Hayden Jananthan<sup>2</sup>, Aydin Buluç<sup>3</sup>, Tim Davis<sup>4</sup>, Daniel Grant<sup>5</sup>, Michael Jones<sup>2</sup>, Chad Meiners<sup>2</sup>, Andrew Morris<sup>5</sup>, Sandeep Pisharody<sup>2</sup>, Jeremy Kepner<sup>2</sup>

<sup>1</sup>University of Arizona, <sup>2</sup>MIT, <sup>3</sup>BNL, <sup>4</sup>Texas A&M, <sup>5</sup>GreyNoise,

**Abstract**— Modern network sensors continuously produce enormous quantities of raw data that are beyond the capacity of human analysts. Cross-correlation of network sensors increases this challenge by enriching every network event with additional metadata. These large volumes of enriched network data present opportunities to statistically characterize network traffic and quickly answer a key question: “What are the primary cyber characteristics of my network data?” The Python GraphBLAS and PyD4M analysis frameworks enable anonymized statistical analysis to be performed quickly and efficiently on very large network data sets. This approach is tested using billions of anonymized network data samples from the largest Internet observatory (CAIDA Telescope) and tens of millions of anonymized records from the largest commercially available background enrichment capability (GreyNoise). The analysis confirms that most of the enriched variables follow expected heavy-tail distributions and that a large fraction of the network traffic is due to a small number of cyber activities. This information can simplify the cyber analysts’ task by enabling prioritization of cyber activities based on statistical prevalence.

**Keywords**— Cybersecurity, High Performing Computing, Big Data, Networks Scanning, Dimensional Analysis, Internet Modeling, Packet Capture, Streaming Graphs.

## I. INTRODUCTION

“What are the primary cyber characteristics of my network data?” is a critical question for anyone protecting a network. Understanding network data characteristics statistically is a powerful tool for prioritizing resources for the most significant cyber activities. Cyber characterization often requires the analysis and correlation of significant volume of network traffic often containing billions of (anonymized) records.

Internet sensors enable the collection of the raw data used to characterize network traffic to help organizations protect cyber assets [1]. This work exhibits large-scale statistical cyber characterization using datasets from the Center for Applied Internet Data Analysis (CAIDA) Telescope and the GreyNoise honeyfarm that is cross-correlated using GraphBLAS (GraphBLAS.org) and Python Dynamic Distributed Dimensional Data Model (d4m.mit.edu) libraries [2].

The CAIDA Telescope passively monitors Internet packets into an internet darkspace that is a globally routed /8 network that is almost entirely adversarial traffic [3]. Honeyfarms are a mechanism for actively observing and interacting with internet traffic to create richer data sets [4]. The GreyNoise honeyfarm consists of hundreds of servers passively collecting packets from IPs scanning the internet. GreyNoise servers have the

additional capability to converse with the IP sources to identify behavior, methods, and intent [5,6]. A significant difference between these two datasets is that CAIDA collects significantly more data over the same period than GreyNoise does – approximately thirty minutes of CAIDA data collection is equivalent to thirty days of GreyNoise data collection. Table I depicts the collected data used for this research. The data from Table I has two start times, GreyNoise and CAIDA. Throughout this paper, the CAIDA start time is used to specify the data collected dates, as seen in Tables II-VI.

Table I. Data collection start time, collection duration, and the number of unique sources from the GreyNoise and CAIDA datasets. GreyNoise data was collected for a month, while CAIDA data was approximately every six weeks on Wednesdays, either at noon or midnight. Constant packet and variable time samples simplify the statistical analysis of the heavy-tail distributions commonly found in network traffic quantities [7].

GreyNoise Start Time	GreyNoise Duration	GreyNoise Sources	CAIDA Start Time	CAIDA Duration	CAIDA Packets	CAIDA Sources
2020-06-01	30 days	1,111,458	20200617-120000	1594 sec	$2^{30}$	670,304
2020-07-01	31 days	1,438,698	20200729-000000	1312 sec	$2^{30}$	541,300
2020-09-01	30 days	1,245,194	20200916-120000	997 sec	$2^{30}$	723,991
2020-10-01	31 days	1,997,782	20201028-000000	1068 sec	$2^{30}$	796,327

The datasets contain network traffic found by collecting data packets from thousands of Internet Protocol (IP) addresses that scan the internet daily. Previous work [7] examined the temporal correlation between CAIDA sources seen by GreyNoise over time, finding that among CAIDA sources that have sent  $d < N_v^{1/2}$  source packets. A modified Cauchy distribution describes the fraction found in GreyNoise sources

$$p(d, t) \propto \frac{\log_2(d)}{\log_2(N_v^{1/2})} \frac{\beta}{\beta + |t - t_0|^\alpha}$$

where  $t$  is the GreyNoise measurement time,  $t_0$  is the CAIDA measurement time,  $N_v$  is the number of CAIDA packets, and  $\alpha$  and  $\beta$  are empirically determined model parameters. In general, 70% of the highest frequency ( $d > N_v^{1/2}$ ) sources in CAIDA are also seen in the same GreyNoise time window.

Building on this prior work, this paper explores in detail the cyber characteristics of the correlated sources that are seen in both data sets. Understanding these characteristics can aid in defending against cyberattacks. The CAIDA telescope darkspace data is rich starting point for this characterization as it represents almost entirely adversarial traffic [8-10]. Previous works made in collaboration with different data collection centers, such as the Widely Integrated Distributed Environment (WIDE) project and CAIDA, have used such characterizations

to understand the global state of Internet traffic and test prototypes to stop internet worms [11,12].

In related work, network characterization can leverage machine learning for anomaly detection, intrusion detection, and behavior analysis[13]. Some machine learning classifiers identify malicious activity prediction with 96% accuracy for intrusion detection even in zero-day exploited vulnerabilities in internet traffic [14]. Likewise, Internet traffic data can be categorized into audio-stream, browsing, P2P, file-transfer, video-stream, and VOIP types based on representative classification features, such as flow duration, time intervals among packets, packet statistics, number of packets, inbound packets, outbound packets, ..., with different analysis applied to each [15-19]. These approaches include convolutional neural networks and bidirectional long short-term memory neural networks to capture local features from the packet's content. Such approaches have resulted in multiclass accuracy of 92% even for encrypted traffic types [20].

CAIDA has been further used to understand internet traffic, in [21-24] addressing the problem of locating the exact Autonomous System Number (ASN), which controls internet routing. In this case, it discriminates traffic by analyzing all possible AS levels and paths by combining measurements from CAIDA; besides analyzing big data traffic using machine learning, it is possible to create systems for intrusion detection. Furthermore, in [25], traffic obtained from CAIDA was used to observe virus and worm behavior over time by applying the approaches mentioned previously.

Prior work has focused on the specific classification of network traffic data, but due to computational limitations, broad statistical characterization on a large scale has been a challenge. This paper demonstrates the feasibility of such characterization on corpora with billions of packets and 100,000s of sources (see Table I). Furthermore, anonymized Internet Protocol (IP) addresses are used to demonstrate that such characterizations can be done with privacy considerations. Working with anonymized IP addresses becomes a powerful aid in data sharing. Anonymizing the IP addresses enables the sharing of the data while keeping the user's information private. The Python GraphBLAS and PyD4M analysis frameworks are key tools to efficiently and effectively perform this analysis on large amounts of anonymized data.

This research addresses the characterization of the cross-correlated CAIDA/GreyNoise data in the following order: Section II presents a dimensional data analysis to determine the variables of interest. Section III develops an “exemplar” record from the most common variables. Section IV computes the probability distributions of selected variables and models them with a 2-parameter Zipf-Mandelbrot distribution. Finally, Section V presents the conclusions of the analysis and future work.

## II. DIMENSIONAL DATA ANALYSIS

Dimensional analysis is used to observe relationships between quantities based on their dimensions in complex systems. Such analysis can be used to understand the information content of the databases and find inconsistencies,

data patterns, and formatting. Relationships do not change when the units of measurement are altered [26]. This concept has been extended to “big data” in the form of dimensional data analysis which looks at size (or dimension) of different values in the data [27]. In this paper, dimensional data analysis of the CAIDA-GreyNoise data helps identify those variables that are amenable to further exploration. Given the amount and type of data being handled, the Python library D4M is used, utilizing the concepts of linear algebra and signal processing to databases through associative arrays while providing a schema capable of representing most data and providing a low barrier to entry through a simple API.

The CAIDA-GreyNoise data is constructed by building GraphBLAS hypersparse traffic matrices for each  $2^{30}$  packet CAIDA sample set listed in Table I. The logarithmically binned number of **source packets**,  $\log_2(d)$ , from each CAIDA source are computed and the source IPs are anonymized using the CryptoPAN protocol. Likewise, the source IPs from the GreyNoise are similarly anonymized allowing the two data sets two be cross-correlated.

The combined CAIDA-GreyNoise variables associated with each anonymized source IP are then separated into three tables based on their dimensional data analysis types: one containing variables that did not need further analysis and two tables with variables that are amenable to further analysis. The latter two tables correspond to how many unique values are associated with those variables, either high (~10,000 or more, Table IV) or low (~10, Table V). The three tables have the same general format with column headings:

**Date:** The start date and time of the CAIDA collection, approximately every six weeks on Wednesday, either at noon (120000) or midnight (000000).

**Variable:** The variable of interest for analysis, collected by CAIDA and GreyNoise.

**Nrow:** Number of source IPs associated with this variable.

**Ncol:** Number of unique values for specific variables.

**Nnz:** Number of nonzero values.

**Maxval:** The value appearing most frequently.

**Maxcount:** The number of times **maxval** appears.

**Maxfrac:** The fraction of the number of times the maximum value appears over each variable's total number of values (i.e.,  $\text{Maxfrac} = \text{Maxcount}/\text{Ncol}$ ). **Maxfrac** is expressed with italics to indicate it can be determined directly from **Maxcount** and **Ncol**.

From the data provided by CAIDA and GreyNoise, the variables chosen for analysis include:

**Actor:** A participant sending the packets over the network.

**ASN:** Autonomous System Number is the number that identifies each autonomous system. It is a collection of connected internet protocol routing prefixes controlled by network operators.

**Classification:** GreyNoise classification of the source IP as unknown, benign, and malicious. A device can be classified as “malicious” if it is flagged as having malicious intent, “benign” if it is without malicious intent, and “unknown” if the purpose of the transmitted packets are unknown.

**CVE:** Common Vulnerabilities and Exposures (CVE) lists publicly known vulnerabilities in devices with related information. Records classified as “benign” or “unknown” do not have a CVE value, while each “malicious” record may have zero or more CVEs associated with it.

**Last seen timestamp** (last seen): The timestamp when GreyNoise last observed the source IP during the one-month observation window.

**OS:** The Operating system (OS) associated with the source IP.

**Protocol port:** network ports associated with communications from the source IP. The port list was truncated at 5 to avoid excessive numbers of ports in the analysis.

**Source packet** (srcPacket): The logarithmically binned  $\log_2(d)$  number of packets from each CAIDA source.

**Source packet No Grey** (caida srcPacket): Same as **source packet** but for those CAIDA source IPs that are *not* found in the GreyNoise data.

**CAIDA Grey Meta** (caidaGreyMeta)/**CAIDA No Grey** (caidaNoGrey): The total values in the matrix for each file, where caidaGreyMeta is the data correlated between GreyNoise and CAIDA and caidaNoGrey is solely obtained from CAIDA.

**Spoofable:** This binary variable identifies whether the source IP has failed to complete a full connection or not.

#### A. Source Variables

Table II is the source table containing more detailed information on the amount of data obtained. The date column shows four dates beginning with the month's year, month, and day number. If a date ends in “120000” the data was collected by CAIDA at noon; however, if the date ends with “000000”, the data was collected at midnight.

Table II. Source table for the data collected on four dates; divided into the year, month, and day of the month. Variables caidaGreyMeta corresponds to source IPs appearing in both GreyNoise and CAIDA datasets, whereas caidaNoGrey corresponds to source IPs appearing in only CAIDA's dataset.

date	variable	nrow	ncol	nnz	max count	maxfrac
20200617-120000	caidaNoGrey	545,980	1	545,980	545,980	1
20200729-000000	caidaNoGrey	394,875	1	394,875	394,875	1
20200916-120000	caidaNoGrey	589,267	1	589,267	589,267	1
20201028-000000	caidaNoGrey	603,273	1	603,273	603,273	1
20200617-120000	caidaGreyMeta	124,300	9	942,112	124,300	0.131
20200729-000000	caidaGreyMeta	146,402	9	1,118,893	146,402	0.130
20200916-120000	caidaGreyMeta	134,699	9	1,034,353	134,699	0.130
20201028-000000	caidaGreyMeta	193,029	9	1,470,649	193,029	0.131

**caidaNoGrey/caidaGreyMeta:** Table II contains the metadata information for CAIDA-GreyNoise cross-correlated records and metadata for CAIDA records with no associated GreyNoise metadata. For caidaGreyMeta, there are nine distinct values representing the variables being analyzed: actor, spoofable, ASN, last seen timestamp, protocol port, os, srcPacket, classification, and CVE. On the other hand, caidaNoGrey shows the one variable caida srcPacket.

#### B. Irrelevant Variables

Table III depicts the variables with a limited number of distinct values that are unlikely to yield additional information.

**Spoofable:** Table III shows a many-to-one correlation between the spoofable packets and the Boolean value “1”. Between 30% - 40% of the source IPs are spoofable though being flagged as spoofable does not necessarily imply that the traffic was spoofed, only that the inverse could not be established. There does not appear to be any major correlation between being flagged as spoofable and the remaining variables. This variable is then irrelevant for further analysis.

**Actor:** Table III shows that there are between 124,300 and 193,029 records found for the actors with a many-to-one correlation; in other words, for each packet, there is a single actor (though this actor may be “unknown”). There are between 22 to 40 unique actors, with the most common actor being “unknown”, showing up about 99% of the time. Because so few records have a ‘known’ actor, this variable is not relevant.

Table III. Irrelevant variables that are unlikely to benefit from further analysis. Variables include actor and spoofable, with the maximum value of actor being “unknown” for any date, while spoofable is a simple binary value.

date	variable	nrow	ncol	nnz	maxval	max count	maxfrac
20200617-120000	spoofable	36,317	1	36,317	1	36,317	1
20200729-000000	spoofable	43,838	1	43,838	1	43,838	1
20200916-120000	spoofable	56,189	1	56,189	1	56,189	1
20201028-000000	spoofable	62,172	1	62,172	1	62,172	1
20200617-120000	actor	124,300	22	124,300	unknown	123,843	0.996
20200729-000000	actor	146,402	26	146,402	unknown	145,812	0.996
20200916-120000	actor	134,699	30	134,699	unknown	133,036	0.987
20201028-000000	actor	193,029	29	193,029	unknown	192,091	0.995

#### C. Relevant Variables

Table IV and Table V are separated by variables with statistical similarities, the size of the number of columns, and, particularly, the number of unique values in the records. Table IV contains the variables with many unique values in the thousands, while Table V contains several unique values in the two digits. Variables in both tables are subsequently analyzed using probability distributions and histograms.

Table IV. Variables related to many (~10,000 and above) unique values, the number of which is represented by ncol. Variables include ASN, last seen timestamp, and port protocol.

date	variable	nrow	ncol	nnz	maxval	max count	maxfrac
20200617-120000	protocol port	124,300	4,021	203,081	TCP/445	44,607	0.219
20200729-000000	protocol port	146,402	4,353	219,650	TCP/445	66,155	0.301
20200916-120000	protocol port	134,699	6,075	210,315	TCP/23	46,874	0.223
20201028-000000	protocol port	193,029	5,541	304,387	TCP/445	78,971	0.259
20200617-120000	ASN	124,300	10,304	124,300	AS4134	6,096	0.049
20200729-000000	ASN	146,402	9,825	146,402	AS3462	8,650	0.059
20200916-120000	ASN	134,699	10,059	134,699	AS17488	130,24	0.097
20201028-000000	ASN	193,029	10,764	193,029	AS4837	118,30	0.061
20200617-120000	last seen	124,300	115,900	124,300	6/23/20 23:20	18	0.000143
20200729-000000	last seen	146,402	130,474	146,402	8/1/20 0:09	16	0.000109
20200916-120000	last seen	134,699	127,504	134,699	10/1/20 0:11	10	0.000074
					10/31/20		
20201028-000000	last seen	193,029	157,549	193,029	23:12	40	0.000207

**Protocol port:** At times, many protocol ports were used for single-packet transmission by a Source IP. The number of protocol ports per record was limited to five for the feasibility of working with the data. The number of unique protocol ports was between 40,000 and 61,000. TCP/445 (SMB) was the most

frequent on three of the collection dates, and TCP/23 (telnet) on 20200916-120000. The most popular protocol port appeared between 21% and 30% of the time.

**ASN:** Each record has one ASN associated with it. There are thousands of distinct ASNs, and there is a different maximum value for each date. The times those maximum values are counted are between 6,096 and 13,024 times, corresponding to between 4.9% and 6.1% of the total of ASNs.

**Last seen timestamp (last seen):** For each given record, there is exactly one last seen timestamp. There are between 115,900 and 157,549 unique last seen timestamps. The maximum values, as expected, are related to the date and time the data was collected. The range count of maximum timestamps is between 10 to 40 or less than 0.02% of the total number of timestamps recorded.

Table V contains variables that are further analyzed. The similarities between these variables are defined by the number of unique values (ncol) being fairly low – between 3 to 36 unique values each.

Table V. Variables exhibiting relatively few unique values (~10), including classification, CVE, os, srcPacket, and srcPacketnoGrey.

date	variable	nrow	ncol	nnz	maxval	max count	Max frac
20200617-120000	CVE	35,695	36	37,150	CVE-2017-0144	33,660	0.906
20200729-000000	CVE	50,241	33	51,546	CVE-2017-0144	48,265	0.936
20200916-120000	CVE	35,271	32	36,500	CVE-2017-0144	32,205	0.882
20201028-000000	CVE	57,274	34	59,252	CVE-2017-0144	52,880	0.892
20200617-120000	classification	124,300	3	124,300	malicious	72,952	0.587
20200729-000000	classification	146,402	3	146,402	malicious	86,058	0.588
20200916-120000	classification	134,699	3	134,699	malicious	86,141	0.639
20201028-000000	classification	193,029	3	193,029	malicious	109,849	0.569
20200617-120000	os	124,300	17	124,300	Windows 7/8	45,107	0.363
20200729-000000	os	146,402	20	146,402	Windows 7/8	68,856	0.470
20200916-120000	os	134,699	31	134,699	Windows 7/8	45,502	0.338
20201028-000000	os	193,029	20	193,029	Windows 7/8	83,013	0.430
20200617-120000	caida srcPacket	545,980	23	545,980	32	104,466	0.191
20200729-000000	caida srcPacket	394,875	24	394,875	32	67,020	0.169
20200916-120000	caida srcPacket	589,267	22	589,267	1	113,371	0.1925
20201028-000000	caida srcPacket	603,273	24	603,273	1	105,623	0.175
20200617-120000	srcPacket	124,300	25	124,300	128	20,570	0.165
20200729-000000	srcPacket	146,402	24	146,402	64	19,750	0.135
20200916-120000	srcPacket	134,699	26	134,699	64	21,907	0.166
20201028-000000	srcPacket	193,029	25	193,029	64	31,783	0.165

**CVE:** Between 35,271 and 57,274 records have a reported CVE; that is between 26% and 30% of the malicious traffic represented, which is less than half of the records. Many CVEs may appear in a single record. The most popular CVE across all dates is CVE-2017-0144. It is a well-known vulnerability called Eternal Blue related to the famous WannaCry attack that became a global problem in 2017 [28]. Between 88% and 93% of the time a CVE was reported.

**Classification:** There are three unique values – “malicious”, “benign”, and “unknown” – for which a “malicious” value represents between 59.6% and 63.95% (72,952 to 109,849 of the records).

**OS:** The number of records with a reported operating system is between 124,300 and 193,029. Every record has a recorded operating system, though this includes “unknown”, which indicates GreyNoise failed to determine the Source IPs

OS. There is a many-to-one relationship between source IPs and OS, with several unique values ranging from 17 to 31 (including “unknown”); see Table IV. The most common OS is Windows 7/8, with a maximum count ranging from 45,107 to 83,013, representing between 33% and 47% of those reported.

**Source packet No Grey (caida srcpacket):** Records with reported source packets range from 39,487 to 60,327. Table IV depicts a many-to-one correlation between source IPs and the (binned) number of source packets found in the CAIDA records. The most common source packet bin size is 1 for two dates and 32-63 for the other two dates. The maximum number of times a specific source packet size range appears is from 67,020 to 113,371 times or 16.98% to 19.24% of the time.

**Source packet (src packet):** Records with reported source packets are between 124,300 and 193,029. Unique sources binned in sizes  $2^n$  range from 23 and 26. Table V exhibits a many-to-one correlation between source IPs and source packet bins; for every entry, there is exactly one source packet range found. The most common source packet size is between 64 and 127 kilobytes and, on one occasion, between 128 and 256 kilobytes. Between 13% to 16.5% of the packets belong to this size range or between 19,750 to 31,783 records.

### III. EXEMPLAR RECORDS

Based on the dimensional data analysis, it is possible to provide an initial answer to the question of “What are the primary cyber characteristics of my network data?” in the form of an exemplar record based on the data’s most common values.

Table VI. Exemplar records reflecting the most frequent value of each variable.

variable	maxval	maxcount	maxfrac	date
actor	unknown	123843	0.996	20200617-120000
	145812	0.996		20200729-000000
	133036	0.988		20200916-120000
	192091	0.995		20201028-000000
CVE	CVE-2017-0144	33660	0.906	20200617-120000
	48265	0.936		20200729-000000
	32205	0.882		20200916-120000
	52880	0.892		20201028-000000
classification	malicious	72952	0.587	20200617-120000
	86058	0.588		20200729-000000
	86141	0.640		20200916-120000
	109849	0.569		20201028-000000
OS	Windows 7/8	45107	0.363	20200617-120000
		68856	0.470	20200729-000000
		45502	0.338	20200916-120000
		83013	0.430	20201028-000000
protocol port	TCP/445	44607	0.220	20200617-120000
	66155	0.301		20200729-000000
	TCP/23	46874	0.223	20200916-120000
	TCP/445	78971	0.259	20201028-000000
source packet noGrey	32	104466	0.191	20200617-120000
		67020	0.170	20200729-000000
	1	113371	0.192	20200916-120000
		105623	0.175	20201028-000000
source packet	128	20570	0.165	20200617-120000
	64	19750	0.135	20200729-000000
		21907	0.163	20200916-120000
		31783	0.165	20201028-000000
ASN	AS4134	6096	0.049	20200617-120000
	AS3462	8650	0.059	20200729-000000
	AS17488	13024	0.097	20200916-120000
	AS4837	11830	0.061	20201028-000000

Table VI the highly frequent values among the variables. An exemplar record based on maxval and maxcount would be 99% of the time, an unknown actor running the Windows 7/8 operating system sending between 64 and 127 packets with malicious intent over TCP/455 with a nonspecific ASN and targets CVE-2017-0144. Such an exemplar record provides a network operators' with highly actionable information about the most common adversarial activities on their network.

#### IV. PROBABILITY DISTRIBUTIONS

While an exemplar record provides an indication of the most common activities, probability distributions shed insight into the broader behavior of the network. Furthermore, many of the variables are consistent with a Zipf-Mandelbrot distribution which allows the characterization of the data with just 2 parameters [29]. The Zipf-Mandelbrot model is denoted by

$$p(d; \alpha, \delta) \propto \frac{1}{(d + \delta)^\alpha}$$

Where  $d$  is the count of the particular value of the variable and  $\delta$  and  $\alpha$  are parameters found using the procedures of [7]. In Figures 1-4, the computed modified Zipf-Mandelbrot model is plotted, noting that the model  $p(d; \alpha, \delta)$  is logarithmically binned before plotting. Figure 1 shows that most source IPs of the network sent around  $10^2$  packets while very few source IPs sent a large number of packets.

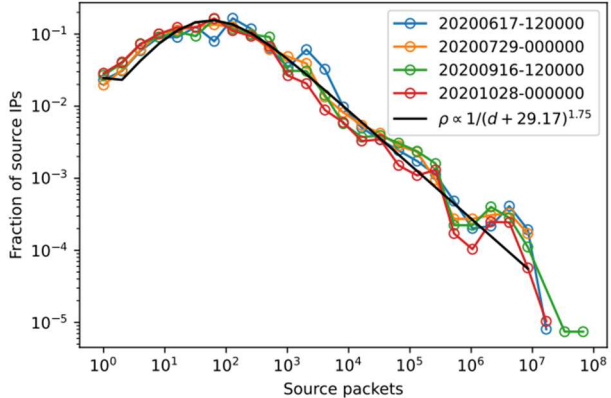


Figure 1. Probability distribution of the fraction of CAIDA source IPs (without GreyNoise matches) versus the number of source packets from the source IP. Most source IPs transmitted between  $10^1$  and  $10^3$  packets. The data are consistent with a Zipf-Mandelbrot distributions with  $\alpha=1.75$  and  $\delta=29.17$ .

Figure 2 has similar behavior to that of Figure 1, in line with the fact that CAIDA and GreyNoise are each observing the similar internet traffic.

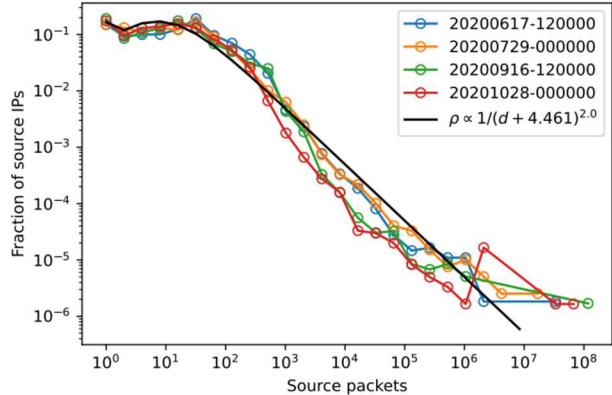


Figure 2. Probability distribution of the fraction of CAIDA source IPs (with GreyNoise matches) versus the number of source packets from the source IP. Most source IPs transmitted less than  $10^2$  packets. The data are consistent with a Zipf-Mandelbrot distributions with  $\alpha=2.0$  and  $\delta=4.461$ . The distribution shows a high number of source IPs with a low number of source packets and a low number of source IPs with a high number of source packets.

The histogram in Figure 3 shows that low-frequency protocol ports represent a higher fraction of the data versus high-frequency ports, suggesting that uncommon protocol ports are favored instead of high-frequency protocol ports by illegitimate traffic.

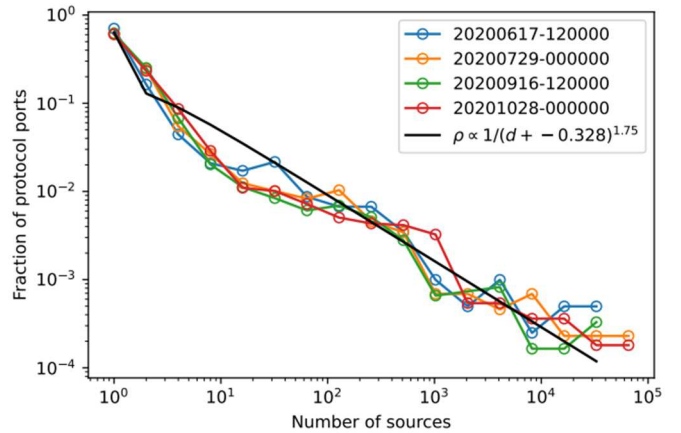


Figure 3. Probability distribution of the fraction of protocol ports versus the number of sources with that protocol port. The data are consistent with a Zipf-Mandelbrot distributions with  $\alpha=1.75$  and  $\delta=-0.328$ . Probability distribution of the number of source IPs versus the fraction of protocol ports utilized by that number of sources. The distribution shows a high number protocol ports used by only a few sources and few protocol ports used by many sources.

The same behavior is seen with ASNs, as in Figure 4, suggesting that uncommon ASNs are favored by illegitimate traffic. Figures 2-4 suggest these variables are relatively consistent over time and consistent with the Zipf-Mandelbrot distributions. These data allow a network operator to prioritize sources based on their impact. Likewise, comparison of new data with the expected distribution can be used to detect changes in behavior which may suggest additional measures.

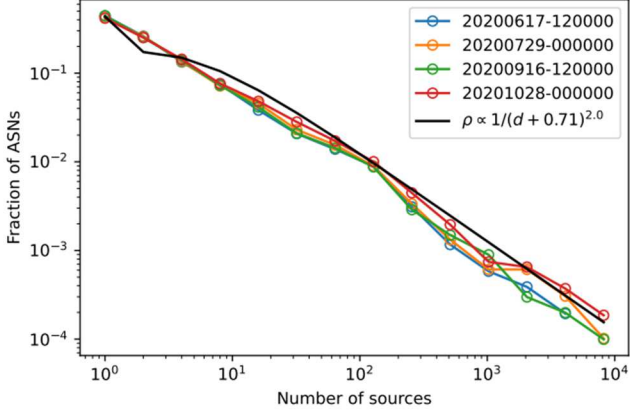


Figure 4. Probability distribution of the fraction of ASNs versus the number of sources with that ASN. The data are consistent with a Zipf-Mandelbrot distributions with  $\alpha=2.0$  and  $\delta=0.72$ . The distribution shows many ASNs were used by only a few sources and few ASNs were used by many sources.

In Figure 5, the correlation between the hour component of the last seen timestamp and the fraction of source IPs last seen at that hour of the day is shown. Lines with 120000 in their label mean the collection started at noon, and those labeled with 000000 were collected at midnight. Data collected at the same time of the day show a close correlation.

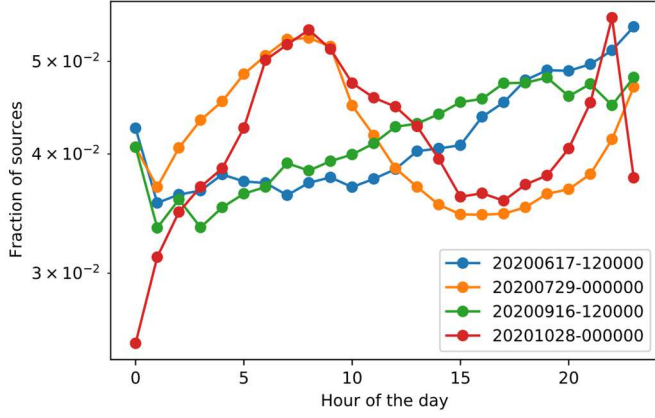


Figure 5. Probability distribution of the hour of the day versus the fraction of source IPs whose last seen timestamp was at that time of day. For the dates ending in 120000, the CAIDA data was collected at noon; for dates ending in 000000, the collection was at midnight. The distributions of last seen timestamps are consistent across those with the same collection times of 120000 or 000000.

The classification distribution in Figure 6 shows that among the three unique values—“benign”, “malicious”, and “unknown”—there are almost no benign packets. Rather, the majority are malicious, and the rest are unknown. The relative frequency is consistent across the four-collection period.

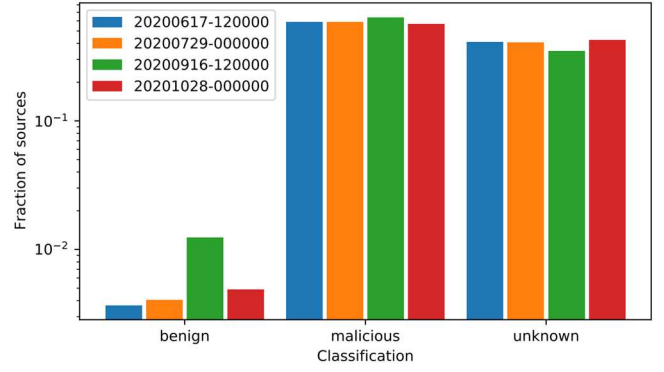


Figure 6. Packet type frequency for CAIDA and GreyNoise. There were three types of classification, with the majority classification for each date being malicious.

Figure 7 shows the distribution of the OSes that is relatively consistent across the four collection periods. While Windows 7/8 was the most common OS from the source IPs, the second most common OS was unknown, followed closely by several versions of Linux. Figure 8 shows a similar trend in time. Both Figure 7 and Figure 8 corroborate the exemplar record shown in Section III, with the most common operating system being Windows 7/8 and the most common CVE being CVE-2017-0144. These are well correlated as the NSA created CVE-2017-0144/Eternal Blue as a windows exploit targeting Microsoft’s implementation of the Server Message Block (SMB) Protocol [27].

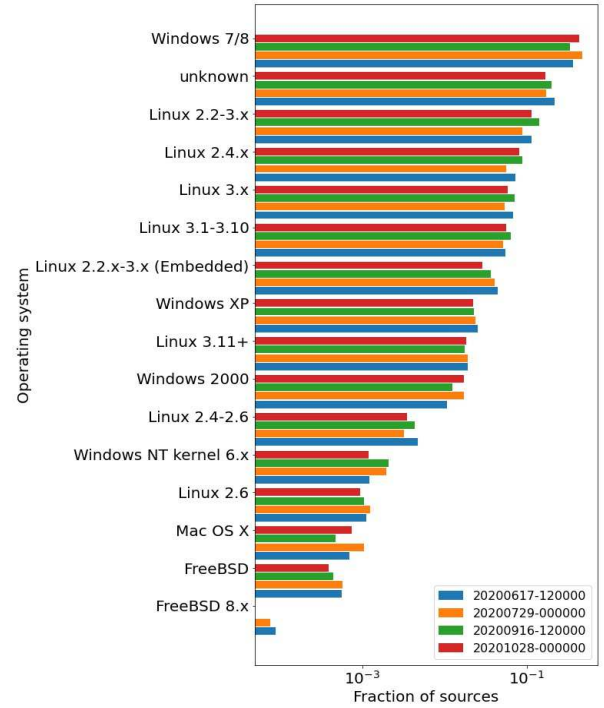


Figure 7. Distribution of the 16 most common operating systems observed by CAIDA and GreyNoise.

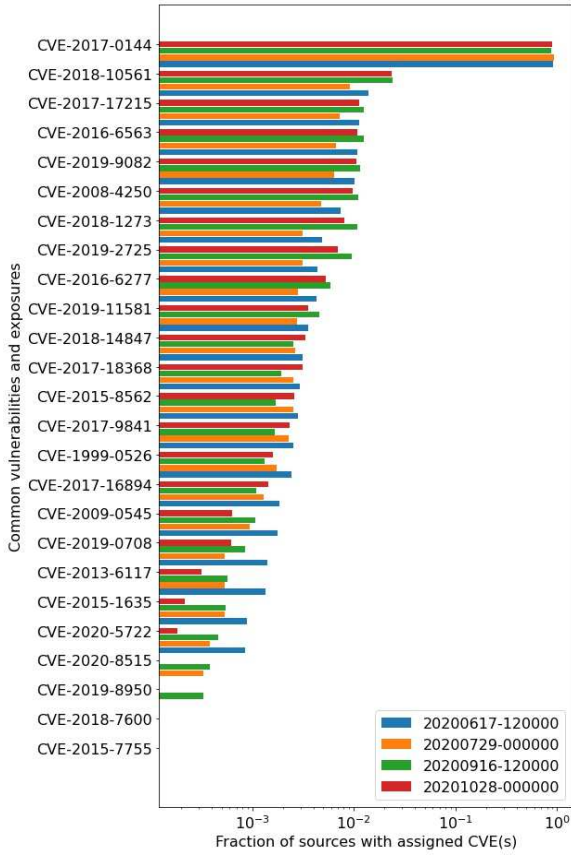


Figure 8. Distribution of the 25 most common CVEs observed by CAIDA and GreyNoise. Data were normalized and arranged in descending order from top to bottom.

## V. CONCLUSIONS AND FUTURE WORK

In this paper, we analyzed a vast amount of raw network traffic from modern sensors by applying correlation to find the main characteristic of the network traffic observed by the CAIDA telescope and GreyNoise honeyfarm. Python GraphBLAS and PyD4M analysis frameworks were used to cross-correlate two datasets from the telescope and a honeyfarm. Hence statistical understanding was obtained, both in terms of dominant characteristics of illegitimate traffic and overall statistical distributions exhibited by the resulting cross-correlated data.

These analyses revealed that certain adversarial activities dominate the traffic – the typical adversary is an unknown actor sending between 64 and 127 packets with malicious intent over protocol port TCP/455 using the Windows 7/8 OS and attempting to utilize CVE-2017-0144/Eternal Blue. As such, cyber defenders should prioritize protection from this adversarial behavior.

Zipf-Mandelbrot distributions model several different phenomena arising from the examined illegitimate traffic, including the packet distribution sent from source IPs as well as the distribution of protocol ports and ASNs among source IPs. A result of these models is that few source IPs send large numbers of packets and that illegitimate traffic highly favors uncommon protocol ports and ASNs.

Due to the previously mentioned, network traffic is caused by small types of cyber activities. Knowing these characteristics, as the typical record, enables focus on the main threats based on statistical occurrences.

Future work will focus on the application of topic modeling techniques – such as sparse nonnegative matrix factorization and truncated singular value decomposition – to the incidence matrices associated with each relevant variable. Such analysis may reveal further information about the dimensionality of the data and the clustering of source IP-variable value pairs.

## VI. ACKNOWLEDGMENTS

The authors wish to acknowledge the following individuals for their contributions and support: Sean Atkins, Bob Bond, Ronisha Carter, K Claffy, Cary Conrad, Tucker Hamilton, Salim Hariri, Bill Hayes, Jeff Gottschalk, Raul Harnasch, Chris Hill, Mike Kanaan, Tim Kraska, Charles Leiserson, Mimi McClure, Sharon Oneal, Christian Prothmann, John Radovan, Steve Rejto, Daniela Rus, Doug Stetson, Scott Weed, Marc Zissman, and the MIT SuperCloud team: Bill Arcand, Bill Bergeron, David Bestor, Chansup Byun, Vijay Gadepally, Michael Houle, Matthew Hubbell, Anna Klein, Joseph McDonald, Peter Michaleas, Lauren Milechin, Julie Mullen, Andrew Prout, Antonio Rosa, Sid Samsi, Albert Reuther, Matthew Weiss, Charles Yee.

This material is based upon work supported by the Assistant Secretary of Defense for Research and Engineering under Air Force Contract No. FA8702-15-D-0001, National Science Foundation CCF-1533644, and United States Air Force Research Laboratory and Air Force Artificial Intelligence Accelerator Cooperative Agreement Number FA8750-19-2-1000. Any opinions, findings, conclusions, or recommendations expressed in this material are those of the author(s) and do not necessarily reflect the views of the Assistant Secretary of Defense for Research and Engineering, the National Science Foundation, or the United States Air Force. The U.S. Government is authorized to reproduce and distribute reprints for Government purposes, notwithstanding any copyright notation herein.

This work is partly supported by the National Science Foundation (NSF) research projects NSF-1624668, (NSF) DUE-1303362 (Scholarship-for-Service, and Department of Energy/National Nuclear Security Administration under Award Number(s) DE-NA0003946. Acknowledgments to CONACyT's Ph.D. fellowship program grant 786773.

In collaboration with the Information Security Research and Education (INSuRE) collaborative, a network of National Centers of Academic Excellence in Cyber Defense Research (CAE-R) universities that cooperate to engage students in solving applied cybersecurity research problems. (Arminda Estrada and Ivan Kawaminami are co-first authors).

## REFERENCES

[1] Houmz, A., Mezzouri, G., Zkik, K., Ghogho, M., & Benbrahim, H. (2021). Detecting the impact of software vulnerability on attacks: A case study of network telescope scans. *Journal of Network and Computer Applications*, 195, 103230. <https://doi.org/10.1016/j.jnca.2021.103230>

[2] Pisharody S., Bernays, J., Gadepally, V., Jones, M., Kepner, J., Meiners, C., Michaleas, P., Tse, A., Stetson, D., "Realizing Forward Defense in the Cyber Domain," 2021 IEEE High Performance Extreme Computing Conference (HPEC), 2021, pp. 1-7, doi: 10.1109/HPEC49654.2021.9622839.

[3] The CAIDA UCSD Network Telescope Traffic Dataset - <2019>, [https://www.caida.org/catalog/datasets/telescope-near-real-time\\_dataset/](https://www.caida.org/catalog/datasets/telescope-near-real-time_dataset/)

[4] Kandanaarachchi, S., Ochiai, H., & Rao, A. (2022). Honeyboost: Boosting honeypot performance with data fusion and anomaly detection. *Expert Systems with Applications*, 201, 117073. <https://doi.org/10.1016/j.eswa.2022.117073>

[5] GreyNoise is the source for understanding internet noise. (n.d.). GreyNoise. Retrieved May 3, 2022, from <https://www.greynoise.io/>

[6] Jiang, X., Xu, D., & Wang, Y. M. (2006). Collapsar: A VM-based honeyfarm and reverse honeyfarm architecture for network attack capture and detention. *Journal of Parallel and Distributed Computing*, 66(9), 1165–1180. <https://doi.org/10.1016/j.jpdc.2006.04.012>

[7] Kepner, J., Jones, M., Anderso, D.Buluç, A., Claffy, B., Davis, T., Arcand, W., Bernays, J., Bestor, D., Bergeron, W., Gadepally, V., Grant, D., Houle, M., Hubbell, M., Jananthan, H., Knein, A., Meiners, C., Milechin, L., Morris, A., Mullen, J., Pisharody, S., Prout, A., Reuther, A., Rosa, A., Siddarth, S., Stetson, D., Yee, C., Michaelas, P. (2022). Temporal Correlation of Internet Observatories and Outposts, Networking and Internet Architecture. <https://doi.org/10.48550/arXiv.2203.10230>

[8] Kepner, J., Jones, M., Andersen, D., Buluc, A., Byun, C., Claffy, K., Davis, T., Arcand, W., Bernays, J., Bestor, D., Bergeron, W., Gadepally, V., Houle, M., Hubbell, M., Klein, A., Meiners, C., Milechin, L., Mullen, J., Pisharody, S., Prout, A., Reuther, A., Rosa, A., Samsi, S., Stetson, D., Tse, A., Yee, C., Michaleas, P. (2021). Spatial Temporal Analysis of 40,000,000,000,000 Internet Darkspace Packets. 2021 IEEE High Performance Extreme Computing Conference (HPEC). <https://doi.org/10.1109/hpec49654.2021.9622790>

[9] Safaei Pour, M., & Bou-Harb, E. (2019). Theoretic derivations of scan detection operating on darknet traffic. *Computer Communications*, 147, 111–121. <https://doi.org/10.1016/j.comcom.2019.08.014>

[10] Kashi Venkatesh Vishwanath and Amin Vahdat. 2006. Realistic and responsive network traffic generation. *SIGCOMM Comput. Commun. Rev.* 36, 4 (October 2006), 111–122. <https://doi.org/10.1145/1151659.1159928>

[11] J. Kepner, K. Cho, K. Claffy, V. Gadepally, P. Michaleas and L. Milechin, "Hypersparse Neural Network Analysis of Large-Scale Internet Traffic," 2019 IEEE High Performance Extreme Computing Conference (HPEC), 2019, pp. 1-11, doi: 10.1109/HPEC.2019.8916263.4

[12] Ferrag, M. A., Maglaras, L., Moschoyiannis, S., & Janicke, H. (2020). Deep learning for cyber security intrusion detection: Approaches, datasets, and comparative study. *Journal of Information Security and Applications*, 50, 102419. <https://doi.org/10.1016/j.jisa.2019.102419>

[13] Q. Zhou and D. Pezaros, "Evaluation of machine learning classifiers for zero-day intrusion detection - an analysis on CIC-AWS-2018 dataset," CoRR, vol. abs/1905.03685, 2019.

[14] Cascavilla, G., Tamburri, D. A., & van den Heuvel, W. J. (2021). Cybercrime threat intelligence: A systematic multi-vocal literature review. *Computers & Security*, 105, 102258.

[15] Lan, J., Liu, X., Li, B., Li, Y., & Geng, T. (2022). DarknetSec: A novel self-attentive deep learning method for darknet traffic classification and application identification. *Computers & Security*, 116, 102663.

[16] Roy, S., Shapira, T., & Shavitt, Y. (2022). Fast and lean encrypted Internet traffic classification. *Computer Communications*, 186, 166–173. <https://doi.org/10.1016/j.comcom.2022.02.003>

[17] Roy, S., Shapira, T., & Shavitt, Y. (2022b). Fast and lean encrypted Internet traffic classification. *Computer Communications*, 186, 166–173. <https://doi.org/10.1016/j.comcom.2022.02.003>

[18] Zhao, J., Jing, X., Yan, Z., & Pedrycz, W. (2021). Network traffic classification for data fusion: A survey. *Information Fusion*, 72, 22–47. <https://doi.org/10.1016/j.inffus.2021.02.009>

[19] Singh, D., Shukla, A., & Sajwan, M. (2021). Deep transfer learning framework for the identification of malicious activities to combat cyberattack. *Future Generation Computer Systems*, 125, 687–697.

[20] Fernández, J., Perez, J., Aguirre, I., Allende, I., Abella, J., & Cazorla, F. J. (2021). Towards functional safety compliance of matrix–matrix multiplication for machine learning-based autonomous systems. *Journal of Systems Architecture*, 121, 102298. <https://doi.org/10.1016/j.sysarc.2021.102298>

[21] Garrett, T., C. E. Bona, L., & P. Duarte, E. (2021b). A Holistic Approach for Locating Traffic Differentiation in the Internet. *Computer Networks*, 200, 108489.

[22] Haldorai, A., Ravana, S. D., Lu, J., & Ramu, A. (2022). Big Data in Intelligent Information Systems. *Mobile Networks and Applications*. <https://doi.org/10.1007/s11036-021-01863-w>

[23] Hardegen, C., Petersen, M., Ezelu, C., Geier, T., Rieger, S., & Buehler, U. (2021). A Hierarchical Architecture and Probabilistic Strategy for Collaborative Intrusion Detection. 2021 IEEE Conference on Communications and Network Security (CNS). <https://doi.org/10.1109/cns53000.2021.9705027>

[24] Meiss, Mark; Menczer, Filippo; Vespiagnani, Alessandro (2011). Properties and Evolution of Internet Traffic Networks from Anonymized Flow Data. *ACM Transactions on Internet Technology*, 10(4), 1–23. doi:10.1145/1944339.1944342.

[25] Hedjam, R., Abdesselam, A., & Melgani, F. (2021). NMF with feature relationship preservation penalty term for clustering problems. *Pattern Recognition*, 112, 107814. <https://doi.org/10.1016/j.patcog.2021.107814>

[26] Xu, Z., Zhang, X., Wang, S., & He, G. (2022). Artificial neural network based response surface for data-driven dimensional analysis. *Journal of Computational Physics*, 459, 111145. <https://doi.org/10.1016/j.jcp.2022.111145>

[27] V. Gadepally and J. Kepner, "Big data dimensional analysis," 2014 IEEE High Performance Extreme Computing Conference (HPEC), 2014, pp. 1–6, doi: 10.1109/HPEC.2014.7040944.

[28] One year after WannaCry: assessing the aftermath. (2018). *Network Security*, 2018(5), 1–2. [https://doi.org/10.1016/s1353-4858\(18\)30037-0](https://doi.org/10.1016/s1353-4858(18)30037-0)

[29] Łapiński, T. M. (2021). Law of large numbers unifying Maxwell–Boltzmann, Bose–Einstein and Zipf–Mandelbort distributions, and related fluctuations. *Physica A: Statistical Mechanics and Its Applications*, 572, 125909. <https://doi.org/10.1016/j.physa.2021.125909>